This is a post-peer-review, pre-copyedit version of an article published in* International Biodeterioration & Biodegradation. *The final authenticated version is available online at: https://doi.org/10.1016/j.ibiod.2018.09.003

Attribution-NonCommercial-NoDerivatives 4.0 International (CC BY-NC-ND 4.0)

Acetylation of *Pinus radiata* delays hydrolytic depolymerisation by the brown-rot fungus *Rhondonia placenta*

Beck, G.*[a, b], Hegnar, O. A.[a, c], Fossdal, C. G.[d], Alfredsen, G.[a]

Declarations of interest: none

*Corresponding author

[a]Norwegian Institute of Bioeconomy Research, Department of Wood Technology, PO Box 115, NO-1431, Ås, Norway

[b]Norwegian University of Life Sciences, Faculty of Environmental Sciences and Natural Resource Management, PO Box 5003, NO-1432, Ås, Norway

[c]Norwegian University of Life Sciences, Faculty of Chemistry Biotechnology & Food Science, PO Box 5003, NO-1432, Ås, Norway

[d]Norwegian Institute of Bioeconomy Research, Department of Forest Health, PO Box 115, NO-1431, Ås, Norway

Abstract

Acetylation of wood can provide protection against wood deteriorating fungi, but the exact degradation mechanism remains unclear. The aim of this study was to determine the effect of acetylation of *Pinus radiata* wood (weight percent gain 13, 17 and 21%) on the expression of genes involved in decay by brown-rot fungus *Rhodonia placenta*. Gene expression analysis using qRT-PCR captured incipient to advanced decay stages. As expected the initiation of decay was delayed as a result the degree of acetylation. However, once decay was established, the rate of degradation in acetylated samples was similar to that of unmodified wood. This suggests a delay in decay rather than an absolute protection threshold at higher acetylation levels. In accordance with previous studies, the oxidative system of *R. placenta* was more active in wood with higher degrees of acetylation and expression of cellulose active enzymes was delayed for acetylated samples compared to untreated samples. The reason for the delay in the latter might be because of the slower diffusion rate in acetylated wood or that partially acetylated cellobiose may be less effective in triggering production of saccharification enzymes. Enzymes involved in hemicellulose and pectin degradation have previously not been focused on in studies of degradation of acetylated wood. Surprisingly, CE16 carbohydrate esterase, assumed to be involved in deacetylation of carbohydrates, was expressed

significantly more in untreated samples compared to highly acetylated samples. We hypothesise that this enzyme might be regulated through a negative feedback system, where acetic acid supresses the expression. The up-regulation of two expansin genes in acetylated samples suggests that their function, to loosen the cell wall, is needed more in acetylated wood due the physical bulking of the cell wall. In this study, we demonstrate that acetylation affects the expression of specific target genes not previously reported, resulting in delayed initiation of decay. Thus, targeting these degradation mechanisms can contribute to improving wood protection systems.

Key words: Acetylated wood, brown-rot decay, gene expression, quantitative real-time PCR.

1. Introduction

Wood is a renewable, natural and carbon sequestering material that requires less energy to manufacture than other nonrenewable construction materials. However, wood's biogenic origin also makes it susceptible to biological degradation. An equivalent of ten percent of the annual timber harvest of the United States is estimated to decay in service each year (Zabel and Morrell 1992). Traditionally, wood decay has been mitigated by impregnation with biocides, but new non-toxic alternative methods are being developed. Acetylation is one such alternative preservation technique.

Rather than relying on the presence of a toxic chemical, acetylation, like other wood modification techniques, imparts decay resistance by chemically altering the wood polymers themselves (Hill 2006). The wood is reacted with acetic anhydride which substitutes the hydrogen of hydroxyl (OH) groups on the wood polymers with an acetyl group and produces acetic acid as a byproduct (Rowell 2005). Acetylation physically bulks the cell wall because of the larger size of the substituted moiety. It has been shown that water is excluded from the acetylated cell wall due to both direct substitution of OH groups leading to less primary sorption sites for water molecules and steric hindrance of unmodified OH groups by the bulky acetyl groups (Papadopoulos and Hill 2003, Popescu et al. 2014, Beck et al. 2017a). In their review article, Ringman et al. (2014a) summarised several prevalent theories of how wood modification methods, such as acetylation, may impart decay resistance: (i) fungal enzymes may become ineffective due to substrate non-recognition, (ii) fungal molecules may not penetrate the modified cell wall due to micropore blocking and/or (iii) diffusion may be inhibited due to low cell wall moisture content. The first theory was rejected because it would not explain hindrance of the initial non-enzymatic degradation of brown-rot fungi. The second also seems unlikely as Hill et al. (2005) demonstrated using solute exclusion that the acetylated cell wall remains accessible to probe molecules up to 4 nm in size. The last theory of diffusion inhibition was identified as the most probable.

In nature, wood is primarily decomposed by basidiomycetous fungi in two polyphyletic groups generally known as white- and brown-rot fungi. White-rot fungi are able to fully degrade cellulose, hemicelluloses and lignin, using a battery of enzymes that act upon the polysaccharides and lignin. Brown-rot fungi on the other hand remove only the polysaccharides but extensively depolymerise and modify lignin before rapidly repolymerising it (Eastwood et al. 2011, Riley et al. 2014).

The main classes of enzymes acting on cellulose in basidiomycetes are endoglucanases belonging to the GH5 and GH12 families, cellobiohydrolases belonging to families GH6 and GH7 and lytic polysaccharide monooxygenases (LPMOs) belonging to the family AA9 (as classified in the Carbohydrate-Active enZYmes database CAZy) (Floudas et al. 2012, Lombard et al. 2013). Hemicellulases play a key role in the enzyme repertoire of these fungi; some species have several dozens of genes encoding mannanases, xylanases, arabinases and glucuronidases. Working in concert with the hemicellulases are carbohydrate esterases that assist in the depolymerisation of wood cell wall polysaccharides through deacetylation. These enzymes, which are generally larger than 50 Å in diameter, are thought to be too large to penetrate the native wood cell wall, where porosity is low (Cowling 1961, Fluornoy et al. 1991). While white-rot fungal genomes generally contain a large number of genes involved in the depolymerisation of cellulose and lignin, brown-rot fungal genomes are surprisingly sparse in comparison (Floudas et al. 2012). One of the brown-rot model fungi *Rhodonia placenta* completely lacks exo-acting cellulases in families GH6 and GH7 and peroxidase genes, and only retains a few endocellulases, and LPMOs, yet is perfectly capable of depolymerising and degrading the cellulose in the wood cell wall (Martinez et al. 2009, Eastwood et al. 2011, Floudas et al. 2012, Riley et al. 2014). Interestingly, the repertoire of hemicellulose acting enzymes is not as limited as the cellulose acting enzymes, implying a particular importance of removing hemicelluloses before efficient cellulose hydrolysis by these fungi.

The apparent lack of a sufficient number of cellulase genes and the wood cell-wall porosity problem is theorised to be circumvented in brown-rot fungi by a non-enzymatic system for wood cell wall depolymerisation that uses iron, oxalic acid and iron-chelating/reducing secondary metabolites (Goodell et al. 1997, Xu and Goodell 2001, Eastwood et al. 2011, Yelle et al. 2011). This system is referred to as the Chelator Mediated Fenton (CMF) system. It is proposed that the fungus chelates iron from the environment and produces reducing compounds as well as hydrogen peroxide, eventually leading to the generation of hydroxyl radicals through the Fenton reaction mechanism within the wood. The fungus alters its local environment by secreting large amounts of oxalic acid, lowering the pH around the hyphae to around 2 while the natural pH of the wood cell wall is approximately 5-6. These high concentrations of oxalic acid are able to chelate iron (Fe^{3+}) from iron-oxide complexes and from the wood. As a consequence of the pH and concentration gradients generated by the high concentration of oxalic acid, the iron is not reduced in the immediate environment of the fungus (Arantes et al. 2012). However, once the iron-oxalate complexes diffuses into the higher pH environment of the wood cell wall, iron-reducing compounds produced by the fungus such as 2,5-dimethoxyhydroquinone will reduce and solubilise the iron (Arantes et al. 2009). Once reduced within the wood cell wall, the iron is able to react with hydrogen peroxide, leading to generation of reactive oxygen species (ROS) (Arantes et al. 2012). It has been known for more than 50 years that strength loss precedes mass loss in brown-rot decayed wood (Cowling 1961). This is due to oxidative depolymerisation via the CMF system, which is employed as a pre-treatment prior to secretion of the hydrolytic enzymes (Arantes et al 2012). These two systems, the oxidative and the hydrolytic, have been shown to be spatially and temporally separated (Zhang et al. 2016).

There are several potential sources for hydrogen peroxide. The genome of *R. placenta* suggests the presence of a number of auxiliary activity enzymes that are known to generate H_2O_2. Among these are AA3 glucose-methanol-choline (GMC) oxidoreductases, AA5 copper radical oxidases and AA7 gluco-oligosaccharide oxidases,

which are able to oxidise a wide variety of compounds present in wood and couple this with the reduction of molecular oxygen, leading to the generation of H_2O_2 (Floudas et al. 2012, Levasseur et al. 2013). AA6 benzoquinone reductases are most likely involved in the reduction and regeneration of catecholate and hydroquinone chelators capable of reducing iron, and are highly expressed during the early stages of brown-rot fungal decay (Jensen et al. 2002, Floudas et al. 2012). Notably, reduced catecholate compounds may also generate hydrogen peroxide under certain conditions, by reducing molecular oxygen. Brown-rot fungi produce several catecholate secondary metabolites, which can potentially penetrate the wood cell wall where they can participate in several of the steps needed for Fenton chemistry to take place (Paszczynski et al. 1999).

To the best of the authors' knowledge, all previous gene expression studies on modified wood are on *R. placenta* and only on a limited number of genes and/or a limited test period. Alfredsen et al. (2016a) compared expression of 25 selected *R. placenta* genes during eight weeks of incubation of unmodified and furfurylated Scots pine sapwood treated to a weight percent gain (WPG) of 14%. Among the findings were confirmed indications of a possible shift toward increased expression, or at least no down regulation, of genes related to oxidative metabolism and concomitant reduction of several genes related to the breakdown of holocellulose in furfurylated wood compared to unmodified wood. Ringman et al. (2014b) compared gene expression of selected genes at incipient decay stages for acetylated, DMDHEU and thermally modified *Pinus sylvestris*. They used *R. placenta* and incubation times up to 8 weeks. For the two selected genes involved in oxidative degradation of holocellulose the pattern between the genes differed, but they generally seemed to be upregulated in modified wood compared to control. The acetylated samples seemed to have a peak in alcohol oxidase expression after two weeks, while the other modifications had the highest expression after eight weeks. For the two genes tested involved in holocellulose degradation, expression levels and trends of the modified wood were similar to those of untreated wood.

Previous studies focusing on acetylated wood include Alfredsen and Pilgård (2014) and Alfredsen et al. (2016b). Alfredsen and Pilgård (2014) tested the effect of leached versus non-leached samples on gene expression of only five genes. No significant differences were found in gene expression after 28 weeks. Alfredsen et al. (2016b) studied *R. placenta* colonisation during 4, 12, 20, 28 and 36 weeks of incubation at three acetylation levels (WPG 12, 17 and 22). The number of expressed gene transcripts was limited (six genes), but the findings supported previous studies where acetylated wood seemed to have some resistance against oxidative mechanisms. This resulted in a delayed decay initiation and slower decay rate. The genes involved in oxidative depolymerisation generally had higher expression levels in acetylated wood than the control. But when comparing the treatments at the same mass loss, a significant difference was only found for two of the genes between 21 %WPG and the control. For the two genes involved in holocellulose depolymerisation, the expression levels were generally higher in the control than in acetylated wood and the highest expression levels in acetylated wood were found after 28 and 36 weeks.

The aim of the present study was determine the effect of acetylation of *Pinus radiata* wood on gene expression of decay related genes by brown-rot fungus *Rhodonia placenta.*. For the first time, incubation periods long enough to allow substantial degradation in highly acetylated wood were provided.

2. Materials and methods

2.1 Wood material

Eight *Pinus radiata* (D. Don) sapwood boards originating from New Zealand were provided by Accsys Technologies. These boards were used to make cylindrical samples (0.6 cm diameter, 1 cm height) according to Beck et al. (2017b). The samples consisted entirely of earlywood in order to get as homogeneous samples as possible. The samples were dried at 103°C for 18 h then cooled down in a desiccator before initial dry weights were recorded. The acetylation procedure was also performed as in the aforementioned study and the three WPG levels were achieved by reacting the wood with acetic anhydride for either 15, 150 or 1750 minutes. No swelling agent was used but the samples were vacuum impregnated with anhydride prior to reaction. Average WPG for the three levels of acetylation were 12.5 ± 1.0% (Ac13), 17.1 ± 0.7% (Ac17) and 21.4 ± 0.7% (Ac21). The acetylated samples were conditioned at 65% relative humidity and 20°C for two weeks before they were sealed in plastic bags and sterilised by gamma irradiation (25 kGY) at the Norwegian Institute for Energy Technology.

2.2 Decay test

Rhodonia placenta FPRL 280 (Fr.) Niemelä, K.H. Larss. & Schigel (also widely known by the now taxonomically invalid name *Postia placenta*) was used to decay the samples. This fungus was chosen because: 1) historically it has been extensively studied as a representative brown-rot fungus (Flournoy et al. 1991; Green III et al. 1992; Winandy and Morrell 1993; Irbe et al. 2006; Niemenmaa et al. 2008; Kim et al. 2009; Martinez et al. 2009; Yelle et al. 2011; Goodell et al. 2017); 2) *R. placenta* was one of the first brown-rot fungi to have its genome sequenced and it is of high quality and well annotated (Martinez et al. 2009); 3) it has been the focus of recent work characterising gene expression (Ringman et al. 2014b; Alfredsen et al. 2016; Presley et al. 2016; Zhang et al. 2016; Zhang and Schilling 2017). This specific strain was used because it is specified in the European decay test standard EN113 (CEN 1997). Until recently, "Ppl" was used as the abbreviation for the protein ID of this species. This identification is kept in the current work to avoid potential misunderstanding. The fungus was first grown on 4% (w/v) malt agar and plugs of actively growing mycelia were transferred to a liquid culture containing 4% (w/v) malt. After two weeks, the liquid culture was homogenised with a tissue homogeniser (Ultra-turrax T25, IKA Werke GmbH & Co. KG, Saufen, Germany) and this mixture was then used to inoculate the samples. Petri dishes (100 x 20 mm) were filled with 20 g soil (2/3 ecological compost soil and 1/3 sandy soil) adjusted to 95% of his water holding capacity according to ENV 807 (CEN 2001) and sterilised at 121°C for 2x60 min. Sterilised plastic mesh was placed on top of the soil and the cylindrical wood samples were placed on top of this mesh with the end grain facing the mesh (8 samples per dish, four replicate plates all of the same acetylation level dedicated to each harvesting point). Each sample was individually inoculated by pipetting 300 µl of the fungal suspension on top of the sample. The samples were incubated at 22°C and 70% relative humidity until they were harvested. The weight of the dishes (including soil and wood specimens) was monitored throughout the incubation period and when total weight dropped below 5 g less than the original weight, 5 ml deionised, sterilised water was added to the soil. Incubation times for analyses in the current study were chosen such that mass losses between the different acetylation levels would be similar at the first harvesting point. The control samples were harvested at weeks 1-4, Ac13 at weeks 2, 4

and 6, Ac17 at weeks 4, 6 and 10 and Ac21 at weeks 10, 16, 24 and 28. Three samples were provided for qRT-PCR analysis and eight samples were weighed for mass loss for each harvesting point. When the samples were harvested, the mycelia covering the surface were carefully removed with a tissue (Delicate Task Wipes, Kintech Science, UK) and then the sample mass was obtained. The eight samples measured for mass loss were then dried for 18 h at 103°C and weighed. The samples provided for qRT-PCR were wrapped individually in aluminium foil and put directly into a container with liquid nitrogen. The samples were then stored at -80°C.

mRNA purification and cDNA synthesis

Wood powder from frozen samples was obtained by cutting the plugs into smaller pieces with a garden shears wiped with 70% alcohol and thereafter Molecular BioProducts™ RNase AWAY™ Surface Decontaminant (Thermo Scientific, Singapore). The wood samples were immediately cooled down again in Eppendorf tubes in liquid nitrogen. Fine wood powder was produced in a Retsch 300 mill (Retsch mbH, Haan, Germany). The wood samples, the 100-mg stainless steel beads (QIAGEN, Hilden, Germany) and the containers were chilled with liquid nitrogen before grinding at maximum speed for 1.5 min. They were then cooled in liquid nitrogen again before a second round of grinding. MasterPure™ Complete DNA and RNA Purification KIT (epicentre, Madison, WI, USA) was used according to the manufacturer's instruction for plant tissue samples with the following exceptions: 1) 90 mg of wood sample; 2) 600 µl tissue and cell lysis solution; 3) incubated at 56°C; 4) added an extra centrifugation step (12000 g, room temperature). NanoDrop™ 2000 spectrophotometer (Thermo Scientific, Singapore) was used to quantify RNA in each sample. To convert RNA to cDNA TaqMan Reverse Transcription Reagent KIT (Thermo Scientific, Singapore) was used according to the manufacturer's instructions. Total reaction volume was 50 µl. 300 ng RNA were reacted with oligo $d(T)_{16}$ primer in RNase free water (Qiagene, Hilden, Germany). The solution was incubated two cycles in the PCR machine (GeneAmp® PCR System 9700, Applied Biosystems, Foster City, CA, USA) at 65 °C/5 min and 4 °C/2 min. The PCR machine was paused and the master mix added. The next three cycles included 37 °C/30 min, 95 °C/5 min and 4 °C/indefinite time. In addition to the test samples, two samples without RNA were added as controls and used for each primer pair. After the cDNA synthesis, 50 µl RNase free water (Qiagene, Hilden, Germany) was added to the samples and mixed well.

2.3 Quantitative Real-time PCR

The qRT-PCR specific primers used to determine the transcript levels of selected genes were designed with a target T_m of 60°C and to yield a 150 base pair product. qRT-PCR was performed using ViiA 7 by Life technologies (Applied Biosystems, Foster City, CA, USA). The master mix included for each sample: 5 µl Fast SYBR®Green Master Mix (Thermo Scientific, Singapore), 0.06 µl 10 µM forward primer, 0.06 µl 10 µM reverse primer, 2.88 µl RNase free water (Qiagene, Hilden, Germany) and 2 µl test sample (total volume 10 µl). The qRT-PCR run included the following stages: Hold stage with initial ramp rate 2.63 °C/s, then 95.0 °C for 20 seconds. PCR stage with 40 cycles of initial ramp rate 2.63 °C/s, 95.0 °C, ramp rate of 2.42 °C followed by 60.0 °C for 20 seconds. The melt curve stage had an initial ramp rate of 2.63 °C/s then 95.0 °C for 15 seconds, ramp rate of 2.42 °C/s 60.0 ° for one second, then 0.05 °C/s. Two constitutive housekeeping genes, β-tubulin - βt (Ppl113871) and α-tubulin - αt (Ppl123093) were used as a baseline for gene expression. The target genes (Tg) and the endogenous controls in this study are listed in Table 1. Protein ID's are according to *Postia placenta* MAD 698-R v1.0 genome,

The Joint Genome Institute (https://genome.jgi.doe.gov/pages/search-for-genes.jsf?organism=Pospl1). Threshold cycle values (C_t) obtained here were used to quantify gene expression. Software used to export the C_t values was QuantStudioTM Real-Time PCR System (Applied Biosystems by Thermo Fiches Scientific, Foster City, CA, USA).

2.4 Quantification of gene expression

C_t-values of βt, αt and Tg were used to quantify gene expression according to Eq. 1:

$$Expression\ level = 10^4 \times 2^{C_t \beta t - C_t Tg} \quad (1)$$

This gives an arbitrary baseline expression of β-tubulin and α-tubulin of 10^4. As an internal control, the expression of βt and αt were compared using the same equation, showing a stable expression, with αt being expressed at approximately 80% relative to βt. Only data for βt was included in this paper.

2.5 Statistical analysis

All statistics were performed in JMP (Version Pro 13, SAS Institute Inc., Cary, NC, USA). Significance of differences in expression levels of each gene were calculated with Tukey's honest significant difference (HSD) test. A probability of ≤0.05 was the statistical type-I error level. Differences were compared between harvesting points within treatment, between the first harvesting points among treatments and between overall expressions of all harvesting points among treatments.

3. Results

3.1 Mass loss and wood moisture content

The mass losses for the acetylated samples are calculated relative to the post-acetylation dry mass and are thus lower compared to unmodified samples due to the added mass from the acetylation (Thybring 2017). Mass loss could also be calculated relative to unmodified wood mass, but we cannot rule out that the fungus may degrade the modification agent along with the wood polymers. Acetyl groups are already present in substantial amounts in unmodified hemicelluloses (Rowell 2005) and *R. placenta* possesses several enzymes with acetyl esterase activity capable of removing these groups (Zhang et al. 2016). Therefore, it is expected that the fungus would, at least partly, degrade the modification chemical with the same biochemistry it uses in unmodified wood and, consequently, fungal growth represented by mass loss is best determined in acetylated samples relative to the modified dry mass.

Mass loss was delayed as a result of acetylation and the initial lag phase increased with the degree of acetylation (Fig. 1). Significant mass loss was first detected after 2 weeks for control samples, 4 weeks for Ac13 samples, 6 weeks for Ac17 and 16 weeks for Ac21 samples. High standard deviations are most likely due to the small size of the test samples and the heterogeneity of the wood. It is important to note that once decay is established, the rate of degradation in acetylated samples is similar to that of unmodified wood. Particularly noteworthy is the high level of degradation achieved in the highly acetylated samples.

The wood moisture content after the last harvesting point was calculated relative to initial dry mass prior to decay, in order to correct for the mass lost during degradation (Thybring 2017). These harvest moisture contents were as follows: control 58.3±8.5% after 4 weeks, Ac13 38.7±9.7% after 6 weeks, Ac17 26.3±2.2% after 10 weeks, Ac21 31.0±6% after 28 weeks. Significantly lower values for acetylated samples compared to controls (Tukey's HSD, $p < 0.05$) indicate the reduced water capacity of the acetylated cell wall.

3.2 Relative gene expression

The mean expression level (n=3) of all selected genes were divided into five groups related to function and summed within each group (Fig. 2). The total summed expression level of the selected genes was lower in all initial harvesting points for the controls and for the three different acetylation levels when compared to later harvesting points. In the control samples at week 1, oxalic acid metabolism and oxidative genes constituted almost 60% of the relative expression. Hemicellulase expression was also relatively high, while the expression of the cellulolytic enzymes remained low. At the first harvesting point for the Ac13 samples, the relative expression of the oxalic acid synthesis genes was lower than the control, while the oxidative genes were at a similar level. The first harvesting point for the Ac17 and Ac21 samples were, on the other hand, dominated by oxidative genes. From 2 to 4 weeks a major up-regulation of the cellulases and hemicellulases was observed, with the relative expression of cellulases increasing over time in the control samples. A similar pattern was also observed in the acetylated samples. Interestingly, the relative expression of the oxidative genes remained high in the Ac21 samples even after 16 weeks when there was significant mass loss, and the relative expression of cellulases did not increase significantly until 24 weeks. Expansin expression was relatively higher in all initial harvesting points for all treatment levels and then showed a relative decrease in expression over time. In the more heavily acetylated samples Ac17 and Ac21, the relative expression of the two selected expansins was higher than in the control and the Ac13 samples.

3.3. Genes involved in oxidative depolymerisation

3.3.1. Oxalate synthesis and oxalate decomposition

Figure 3 illustrates the two genes presumed to be involved in oxalic acid synthesis in *R. placenta* – glyoxylate dehydrogenase (GlyD Ppl121561) and oxaloacetate dehydrogenase (OahA Ppl112832) and one involved in oxalic acid degradation – oxalate decarboxylate (OxaD Ppl43912). No significant trends were observed in the expression levels of GlyD and OahA, except for a significant up-regulation for Ac17 w4 compared to w10.

The expression levels of OxaD were very low and should be interpreted with caution. Among the harvesting points within treatment, both Ac17 and Ac21 showed significant up-regulation for this gene at later harvesting points compared to early ones.

3.3.2 Redox enzymes

Figure 4 illustrates six genes assumed to be involved in processes of oxidative brown-rot decay, including three GMC oxidoreductases (AOx1 Ppl44331, AOx2 Ppl129158 and

AOx3 Ppl118723), two copper radical oxidases (Cro1 Ppl56703, Cro2 Ppl104114) and a benzoquinone reductase (BqR Ppl12517).

In unmodified samples no significant up-regulation was observed during early decay for any of the GMC oxidoreductases or copper radical oxidases. The only significant difference between harvesting points for unmodified samples was an up-regulation during late decay (w4 vs. w1 and w2) for AOx2. Interestingly, the GMC oxidoreductases and copper radical oxidases did not show a co-regulated expression pattern. BqR showed no significant difference between harvesting points.

Several of the genes involved in oxidative chemistry showed different expression patterns for acetylated samples compared to controls. AOx2 is significantly up-regulated in acetylated samples compared to unmodified samples when comparing the treatments at the initial decay harvesting point and when all harvesting points are pooled. Moreover, pooled harvesting point expression of AOx3 was significantly higher in Ac17 and Ac21 compared to controls and initial decay expression of Cro1 in Ac21 was significantly up-regulated compared to other treatments.

3.4 Hydrolytic enzymes involved in polysaccharide depolymerisation and LPMO

3.4.1 Cellulose degradation

Figure 5 illustrates selected cellulose degrading enzymes. Expression levels of the three endocellulases (Cel5a Ppl115648, Cel5b Ppl103675 and Cel12a Ppl121191) and the betaglucosidase (bGlu Ppl128500) were delayed, with close to no transcription at the first harvesting points in both unmodified and acetylated samples. For Cel5a and Cel5b, expression at the initial harvesting point was significantly lower than later harvesting points for controls and acetylated samples (except Cel5b Ac21). Cel12a also showed significantly lower expression at the first harvesting point for Ac13 and Ac17 and bGlu expression was significantly lower at earlier incubation times for unmodified and Ac13 samples. Expression of these cellulose active enzymes was delayed for acetylated samples compared to controls. For Ac21, expression levels of Cel5a, Cel5b, Cel12a and the LPMO were still negligible at 10 weeks of decay.

Generally, the *R. placenta* cellulose active enzymes showed lower levels of expression at higher levels of acetylation. Overall expression levels of pooled harvesting points for Cel5a and Cel12a were significantly reduced for Ac21 compared to Ac13 and bGlu was significantly reduced for Ac21 compared to both Ac13 and controls.

We were only able to detect expression of a single LPMO (Ppl126811). Unlike the other cellulose active enzymes which showed a tendency for down-regulation in acetylated samples, no significant differences were found in LPMO expression levels between treatments (Fig. 5). Within treatment, there was a significant up-regulation at the second harvesting point compared to the first harvesting point for Control, Ac17 and Ac21 samples. In control samples, this expression pattern correlates well with the expression of Cel5a and lags slightly behind that of bGlu.

3.4.2. Hemicellulose and pectin degradation

Figure 6 illustrates expression of hemicellulose and pectin active enzymes. Expression levels of Man5a (Ppl121831) and the two endoxylanases (Xyl10a Ppl113670 , Xyl10b Ppl105534) showed a similar trend within the control samples where the first harvesting point was down-regulated when compared to later harvesting points. This expression pattern for control samples is similar to Cel5a and Cel5b (Fig. 5) but relative expression levels are higher in the hemicellulases, particularly at the first harvesting point. CE16a (Ppl125801) expression in control samples followed the same pattern as Man5a, Xyl10a and Xyl10b showing a significant down-regulation at the first harvesting point compared to later harvesting points. There were no significant changes in expression levels of bXyl (Ppl51213) for control samples throughout degradation, but values tended to be higher at later harvesting points. Expression levels of Gal28a (Ppl111730) were up-regulated during the first harvesting point compared to later harvesting points for control samples.

The effect of acetylation on the level of hemicellulose and pectin active enzyme transcripts was variable. Both overall expression and expression level at the first harvesting point were up-regulated in control samples compared to all acetylated samples for Man5a, but no significant differences were observed for Xyl10a and Xyl10b. Comparison of expression levels of Gal28a at the first harvesting point showed significant up-regulation in control samples compared to all acetylated samples. Overall CE16a expression levels were significantly higher in control samples compared to Ac21.

3.5. Expansins

Figure 7 illustrates the two selected genes predicted to encode expansins (Exp1 Ppl126976 and Exp2 Ppl128179). The expression of the two expansins was highly variable and no general trends were observed in unmodified samples at the various stages of decay. Overall expression levels of pooled harvesting points for Exp1 were up-regulated in Ac13 compared to the other treatments and for Exp2 they were up-regulated in all acetylated samples compared to control samples.

4. Discussion

4.1 Mass loss and wood moisture content

Much of the literature on decay of acetylated wood claims that acetylation of around 20% WPG infers complete resistance to fungal degradation (Goldstein et al. 1961; Peterson and Thompson 1978; Kumar and Agarwal 1983; Takahashi et al. 1989; Beckers et al. 1994; Papadopoulos and Hill 2002; Mohebby 2003; Hill et al. 2006). However, as suggested by Hill (2006), this protection threshold may only be present due to the insufficient timeframe of the standard decay experiments employed. Studies using longer decay periods (>250 days) have shown low but observable mass loss (<5%) for 20 % WPG acetylated wood decayed with *R. placenta*, which indicates that decay is not fully inhibited by the modification but rather delayed (Alfredsen et al. 2016b, Ringman et al. 2017). The results of this study confirm this delay for brown-rot degradation in acetylated wood. However, the mass losses obtained for highly acetylated samples reported here are much higher than those of the aforementioned studies which used even longer decay periods (Fig. 1). The smaller wood sample dimensions used in the current study provide a possible explanation for the much higher mass losses reported. The higher surface area to volume ratio of smaller samples may facilitate diffusion of water into the wood cell walls and thus promote fungal degradation.

The acetylated cell wall has reduced water capacity compared to the native wood cell wall (Papadopoulos and Hill 2003, Popescu et al. 2014, Passarini et al. 2017, Beck et al. 2017b). Lower wood moisture contents after the last harvesting point for more highly acetylated samples indicate this reduced water capacity.

4.2 Relative gene expression

For the unmodified wood samples at the first harvesting point, the relatively high hemicellulase expression indicates that the fungus most likely was in a transitional phase from oxidative degradation to hydrolytic depolymerisation, while the expression of the cellulolytic enzymes remained relatively low (Fig. 2). Up-regulation of hemicellulases prior to cellulases in control samples is in agreement with previous observations that hemicelluloses are selectively removed prior to cellulose in brown-rot decayed wood (Winandy and Morrell 1993, Irbe et al. 2006). This trend was also observed in the acetylated samples.

The oxidative genes were highly represented at the first harvesting point for the Ac17 and Ac21 samples which may suggest that the fungus was still in the oxidative pre-treatment stage of decay. For the Ac21 samples, reduction in the relative expression levels of oxidative genes did not occur until week 24. Here it is important to note that the major contributor to this relative high expression in these particular samples was AOx3 (93% of the expression in the oxidative category). This GMC oxidoreductase shows a high degree of similarity to known methanol oxidases (Waterham et al. 1997). We hypothesise that acetylation leads to an increased need for oxidative depolymerisation, and that this oxidative attack more severely demethoxylates lignin, generating methanol. AOx3 would then oxidise and detoxify the methanol, generating H_2O_2 as a by-product (Filley et al. 2002, Niemenmaa et al. 2008).

Expansin expression was relatively higher in the Ac17 and Ac21 samples at the first harvesting point in comparison to Ac13 and control samples. A possible explanation for this is an increased need for opening of the wood cell-wall structure due to the increased bulking caused by acetylation.

4.3. Genes involved in oxidative depolymerisation

4.3.1. Oxalate synthesis and oxalate decomposition

Brown-rot fungi are known to secrete organic acids, including oxalic acid. Calcium oxalate crystals have been found in furfurylated wood (Alfredsen et al. 2016a), thermally modified and acetylated wood (Pilgård et al. 2017). Oxalic acid is, according to Arantes and Goodell (2014), assumed to play an important role as an iron chelator and a phase transfer agent in the CMF system. The selected genes have previously been shown to be regulated spatially during decay by *P. placenta* MAD-698, with the GlyD and OahA being up-regulated at the hyphal front and OxaD up-regulated in older parts of the hyphae (Zhang et al. 2016). Alfredsen et al. (2016) studied five genes involved in oxalic acid metabolism after 2-8 weeks of incubation and found no statistically significant changes in gene expression during *R. placenta* decay in *P. sylvestris* sapwood. The lack of statistical trends in that study and the results presented here for up-regulation of genes involved in oxalic acid synthesis (GlyD and OahA) during the early decay stage (except

Ac17, Fig. 3) may be because the harvesting points selected did not capture the early peak of expression. Zhang et al. (2016) showed that after only 48 hours of growth, *R. placenta* has already begun the transition from oxidative pre-treatment to enzymatic polysaccharide hydrolysis. This suggests that the shortest incubation time of the present study (1 week) may not capture this oxidative behaviour. Later expression of OxaD agrees with the results of Zhang et al. (2016) and affirms the role of this enzyme in oxalic acid decomposition.

4.3.2 Redox enzymes

GMC oxidoreductases (CAZy family AA3) are a family of flavoenzymes that oxidise aliphatic alcohols, aryl alcohols and mono- and disaccharides. This oxidation is coupled with the reduction of a variety of electron acceptors, including O_2 (resulting in the formation of H_2O_2), quinones or other enzymes (such as LPMOs) (Sützl et al. 2018). Copper radical oxidases (CAZy family AA5) are known to be a major constituent of the secretome of several brown rot fungi (Kersten and Cullen 2014). They oxidise a variety of substrates, with the concurrent production of H_2O_2 via the reduction of O_2. Benzoquinone reductases (CAZy family AA6) are intracellular enzymes that protect the fungus from toxic compounds, but have also been suggested to contribute to a non-enzymatic depolymerisation of wood cell wall components by mediating the regeneration/reduction of catecholate iron chelators (Jensen et al. 2002).

It has been suggested that the role of GMC oxidoreductases and copper radical oxidases during brown-rot decay is to generate H_2O_2 which reacts with ferrous iron in the CMF system during initial oxidative degradation (Arantes and Goodell 2014). In unmodified samples no significant up-regulation was observed in this study during early decay for any of the five members analysed in these two families (Fig. 4). Zhang and Schilling (2017) found gradual up-regulation of AOx3 and Cro1 in *R. placenta* incubated on spruce media for 70 hours and Zhang et al. (2016) reported up-regulation of the same genes at the hyphal front compared to older parts of the hyphae for *R. placenta* grown on solid spruce wood. As mentioned previously, the first harvesting point used in this study may have failed to capture the early oxidation behaviour. Alfredsen et al. (2016b) and Ringman et al. (2014b) were also unable to find any significant differences in *R. placenta* degraded Scots pine sapwood between 2 week and 8 week harvesting points for AOx3.

The lack of co-regulation of the enzymes in the GMC oxidoreductase and copper radical oxidase families suggests different roles for the individual enzymes within the same families. H_2O_2 is known to be damaging to enzymes, and the current paradigm suggests that the oxidative and the hydrolytic systems need to be spatially separated. Up-regulation of AOx2 during later decay stages may suggest that this particular enzyme does not produce H_2O_2, but instead detoxifies and reduces quinone derived compounds, potentially serving as Fe^{3+} reductants, thereby regenerating them in a similar manner to benzoquinone reductases (Jensen et al. 2002, Cohen et al. 2004, Arantes and Goodell 2014). It is important to note here that even though several of the genes chosen here have a proposed function, they are not as well characterised and understood as those involved in hydrolytic depolymerisation.

Higher expression levels of redox enzymes in samples with higher degrees of acetylation suggest that the oxidative system of *R. placenta* is more active in acetylated wood. This is in accordance with previous work which has shown up-regulation of redox enzymes in

both acetylated (Alfredsen and Pilgård 2014, Alfredsen et al. 2016b,) and chemically modified wood (Alfredsen and Fossdal 2009, Ringman et al. 2014b, Alfredsen et al. 2016a). The reduced water capacity of the acetylated cell wall (Papadopoulos and Hill 2003, Popescu et al. 2014, Passarini et al. 2017, Beck et al. 2017b) will reduce the rate of diffusion into it and may hinder the oxidative system. Since it appears that the transition from oxidative degradation to enzymatic hydrolysis is triggered by the presence of degradation products like cellobiose (Zhang and Schilling 2017) which must diffuse out of the cell wall (Goodell et al. 2017), the slower diffusion rate in acetylated wood may delay the signal to switch between the two systems.

4.4 Hydrolytic enzymes involved in polysaccharide depolymerisation and LPMO

4.4.1 Cellulose degradation

The two endoglucanases, Cel5a and Cel5b, cause chain breaks in amorphous cellulose. In addition, we chose one endoglucanase, Cel12a, in CAZy family GH12 that, based on sequence similarity, is most likely an endocellulase. The *R. placenta* genome contains no known processive cellulases (cellobiohydrolases), and it is not well understood how the depolymerisation of cellulose to cellobiose by *R. placenta* occurs. One possibility is that its endocellulases can hydrolyse soluble short chain cellulose oligomers that have been generated via the oxidative mechanism. Betaglucosidases (CAZY family GH3) are enzymes that release glucose from the non-reducing end of disaccharides and oligosaccharides and play a key role in all wood decaying organisms, as they catalyse the final glucose producing step. We chose one cellobiose active betaglucosidase, bGlu, and one xylobiose active betaglucosidase, bXyl (see next section), from family GH3 that are known to be highly expressed by *R. placenta* (Zhang et al. 2016).

Higher expression levels during later decay for the cellulose degradating enzymes observed in this study (Fig. 5) agrees with the theory that enzymatic saccharification is segregated from the potentially damaging CMF system (Arantes et al. 2012, Zhang et al. 2016).

Higher levels of acetylation resulted in lower levels of expression for the cellulose active enzymes. Zhang and Schilling (2017) showed that the transcription of these cellulase genes is induced by the presence of cellobiose. In highly acetylated samples, mass loss includes not only the degraded wood polysaccharides capable of producing cellobiose, but also the added mass of the acetyl groups. This may contribute to lower cellobiose concentration at equivalent levels of mass loss for more highly acetylated samples. Additionally, some of the cellobiose produced via oxidative degradation in acetylated samples may remain partially acetylated. This acetylated cellobiose may be less effective in triggering production of saccharification enzymes.

The delayed expression of cellulolytic enzymes and concurrent delayed mass loss in highly acetylated samples raises the question of what nutrient source the fungus is utilising during this period of apparent inactivity. Some nutrition may be available to the fungus from the soil in the Petri dish. Brown rot fungi have been shown to translocate calcium and magnesium from forest soils into woody debris (Smith et al. 2007, Schilling and Bissonnette 2008). It seems the fungus is able to sustain the oxidative system in highly acetylated wood with only the limited amount of nutrition available to it in the soil.

LPMOs are a class of oxidative enzymes that are known to cause chain breaks in crystalline and amorphous regions of both cellulose and hemicelluloses. Eukaryotic LPMOs are placed in CAZy auxiliary activity families 9, 11, 13 and 14, with AA9s showing activity on both cellulose and hemicelluloses. The *R. placenta* genome contains two AA9s (Martinez et al. 2009, Zhang et al. 2016), but we were only able to detect expression of a single one (Ppl126811). Although the expression level is several orders of magnitude lower than the classical cellulases, AA9s are known to play a major role as catalysts of efficient cellulose depolymerisation (Hemsworth et al. 2015). No significant differences were found between treatments for expression levels of the LPMO assessed here. This suggests that LPMO expression may not be regulated by the same mechanism as the other enzymes, or that the expression levels were too low to detect any significant differences. Whether cellobiose, which induces the expression of Cel5a, Cel5b, Cel12a and bGlu (Zhang and Schilling 2017), also controls LPMO expression is not known. LPMOs, like other cellulolytic enzymes, are sensitive to H_2O_2 and will be deactivated in the presence of high ROS concentrations. Thus, they also need to be separated from the oxidative system.

In control samples, the LPMO expression levels correlate with those of Cel5a and lag slightly behind those of bGlu. Coordinated expression of the LPMO with Cel5a affirms the auxiliary role of the LPMO. Betaglucosidase, which showed highest expression levels after three weeks in the control samples, reflects a high production of soluble cellulose oligomers at this stage.

4.4.2. Hemicellulose and pectin degradation

In addition to the limited set of cellulases, the *R. placenta* genome also contains a suite of hemicellulases that attack and depolymerise a wide variety of polysaccharides, including xylans, mannans and other glucans. In this study, we assessed one endomannanase in CAZy family GH5 (Man5a), two endoxylanases in CAZy family GH10 (Xyl10a and Xyl10b) and one betaxylosidase in CAZy family GH3 (bXyl). Enzymes capable of deacetylating polysaccharides were of particular interest for this study. We selected several carbohydrate esterases, but were only able to detect expression of one in CAZy family CE16 (CE16a). Esterases in family CE16 are polysaccharide esterases known to deacetylate xylans and glucans (Li et al. 2008, Zhang et al. 2011). The *R. placenta* genome does not contain any carbohydrate esterases in the well characterised families CE1 and CE2 (Martinez et al. 2009).

For control samples, Man5a, Xyl10a, Xyl10b and CE16a were down-regulated at the first harvesting point and showed coordinated up-regulation at later harvest points (Fig. 6). This coordinated expression indicates the synergistic role of CE16a in deacetylating the hemicelluloses to facilitate their hydrolysis by the hemicellulase enzymes.

Based on previously published work by Zhang et al. (2016), we selected a polygalacturonase in CAZy family GH28 that is highly expressed during decay (Gal28a). Brown-rot fungi have been shown to rapidly degrade pectin during incipient decay because it is a readily available carbohydrate and its removal from pit membranes allows the fungus to further colonise the wood (Tschernitz and Sachs 1975, Green III et al. 1996). With its high galacturonic acid content, pectin is highly vulnerable to hydrolysis by Gal28a. Thus, the up-regulation of this gene during early decay gives access to an important carbon source when the other carbohydrates remain inaccessible.

Comparing acetylated samples to control samples, both overall expression and expression level at the first harvesting point were up-regulated in all acetylated samples compared to controls for Man5a, while no significant differences were observed for Xyl10a and Xyl10b. Zhang and Schilling (2017) showed Man5a was strongly up-regulated in the presence of cellobiose compared to no carbon source controls, while Xyl10a expression was unaffected by cellobiose and Xyl10b expression was only significantly up-regulated by cellobiose during the first 24 h of incubation. The effect of acetylation on cellobiose concentration discussed previously in section 4.4.1 may explain the significant down-regulation of Man5a in acetylated samples.

Pectin may be degraded by the sustained high temperature used during the acetylation reaction. Thus, less available pectin in acetylated samples may explain the lower expression levels of Gal28a compared to controls. As mentioned above, pectin might serve as an important initial carbon source, thus if some is removed during treatment this will further inhibit initial fungal growth.

The fact that overall expression levels of CE16a were significantly higher in control samples than in Ac21 samples was surprising. With higher acetylation levels one might expect up-regulation of enzymes capable of deacetylating wood polysaccharides. It was hypothesised that these enzymes would be part of the machinery involved in deacetylating the wood polymers facilitating hemicellulase and cellulase degradation. Deacetylation of the wood polymers is necessary for the cellulase and hemicellulase enzymes to function most efficiently, and a negative impact of cellulose acetylation has been reported (Pan et al. 2006). However, Ringman et al. (2015) showed that cellulase enzymes are still capable of degradating acetylated substrates, and it has even been suggested that under certain conditions acetylation will actually improve saccharification of the cellulose polymer (Olaru et al. 2011). Furthermore, deacetylation may still occur in acetylated wood but it may happen during initial oxidative degradation. We hypothesise that CE16a is regulated through a negative feedback system, where acetic acid, potentially produced via deacetylation during oxidative degradation, supresses CE16a expression.

4.5. Expansins

Expansins are enigmatic proteins with no known catalytic activity involved in cell wall loosening that synergistically increase the depolymerisation of wood cell wall components when acting in concert with cellulases and hemicellulases. They are believed to increase enzyme access by loosening plant cell-wall interactions (Rose & Bennett 1999, Baker et al. 2000, Arantes & Saddler 2010). The significantly higher expression levels observed for the two expansin genes (Fig. 7) and the higher relative expression for the expansin group (Fig. 2) compared to control samples suggest the fungus may up-regulate expression of these enzymes to cope with the lower cell wall nanoporsity in acetylated wood (Hill et al. 2005).

Conclusion

As previously reported, the expression of oxidative genes of *R. placenta* was upregulated in wood with higher degrees of acetylation and the expression of cellulose active genes was delayed for acetylated samples compared to untreated samples. The delay observed for cellulose active enzymes could be due to the slower diffusion rate in acetylated wood

or that acetylated cellobiose is less effective in triggering production of the saccharification enzymes. The gene expression analysis revealed differential expression of selected genes not previously reported. We demonstrate specific upregulation of expansins believed to be involved in creating access to acetylated wood cell wall components. The studied carbohydrate esterase appeared to be under the influence of a negative feedback system.

Acknowledgments

Sigrun Kolstad and Inger Heldal are acknowledged for molecular analyses. This project was financed by NIBIO (PhD scholarship project no. 335006) and The Research Council of Norway 243663/E50 BioMim.

References

Alfredsen, G., Fossdal, C.G., 2009. *Postia placenta* gene expression of oxidative and carbohydrate metabolism related genes during growth in furfurylated wood. IRG/WP 09-10701. The International Research Group on Wood Protection, Stockholm, Sweden.

Alfredsen, G., Pilgård, A., 2014. *Postia placenta* decay of acetic anhydride modified wood – effect of leaching. Wood Material Science & Engineering 9(3), 162-169.

Alfredsen, G., Fossdal, C.G., Nagy, N.E., Jellison J., Goodell, B., 2016a. Furfurylated wood - impact on *Postia placenta* gene expression and oxalate crystal formation. Holzforchung 70(10), 947-962.

Alfredsen, G., Pilgård, A., Fossdal, C.G., 2016b. Characterisation of *Postia placenta* colonisation during 36 weeks in acetylated southern yellow pine sapwood at three acetylation levels including genomic DNA and gene expression quantification of the fungus. Holzforschung 70(11), 1055-1065.

Arantes, V., Goodell, B. (2014). Current understanding of brown-rot fungal biodegradation mechanisms: a review. In Deterioration and Protection of Sustainable Biomaterials (Vol. 1158, 3–21). American Chemical Society.

Arantes, V., Jellison, J., Goodell, B. (2012). Peculiarities of brown-rot fungi and biochemical Fenton reaction with regard to their potential as a model for bioprocessing biomass. Applied Microbiology and Biotechnology, 94(2), 323-338.

Arantes, V., Qian Y., Milagres, A.M., Jellison J., Goodell, B. 2009. Effect of pH and oxalic acid on the reduction of Fe 3+ by a biomimetic chelator and on Fe 3+ desorption/adsorption onto wood: Implications for brown-rot decay. International Biodeterioration & Biodegradation 63(4), 478-83.

Arantes, V., Saddler, J. N., 2010. Access to cellulose limits the efficiency of enzymatic hydrolysis: the role of amorphogenesis. Biotechnology for biofuels 3(1), 4.

Baker, J.O., King, M.R., Adney, W.S., Decker, S.R., Vinzant, T.B., Lantz, S.E., Nieves, R.E., Thomas S.R., Li, L-C, Cosgrove D.J., Himmel, M.E., 2000. Investigation of the cell-wall loosening protein expansin as a possible additive in the enzymatic saccharification of lignocellulosic biomass. In: Finkelstein M., Davidson B.H. (Eds.), Twenty-First Symposium on Biotechnology for Fuels and Chemicals. Applied Biochemistry and Biotechnology. Humana Press, Totowa, NJ, USA, pp. 217-223.

Beck, G., Strohbusch, S., Larnøy, E., Militz, H., Hill, C.A.S., 2017a. Accessibility of hydroxyl groups in anhydride modified wood as measured by deuterium exchange and saponification. Holzforschung 72(1), 17-23.

Beck, G., Thybring, E.E., Thygesen, L.G., Hill, C.A.S., 2017b. Characterisation of moisture in acetylated and propionylated radiata pine using low-field nuclear magnetic resonance (LFNMR) relaxometry. Holzforschung 72(3), 225-233.

Beckers, E.P.J., Militz, H., Stevens, M., 1994. Resistance of wood to basidiomycetes, soft rot and blue stain. IRG/WP 94-40021. The International Research Group on Wood Protection. Stockholm, Sweden.

CEN (1997) EN113. Wood preservatives - Test method for determining the protective effectiveness against wood destroying basidiomycetes. Determination of the toxic values. CEN (European committee for standardization), Brussels.

CEN (2001) ENV807. Wood preservatives - Determination of the effectiveness against soft rotting micro-fungi and other soil inhabiting micro-organisms. CEN (European committee for standardization), Brussels.

Cowling, E.B., 1961. Comparative biochemistry of the decay of sweetgum sapwood by white-rot and brown-rot fungi. No. 1258. US Dept. of Agriculture. Washington, USA.

Cohen, R., Suzuki, M.R., Hammel, K.E., 2004. Differential stress-induced regulation of two quinone reductases in the brown rot basidiomycete *Gloeophyllum trabeum*. Applied and environmental microbiology 70(1), 324-331.

Eastwood, D.C., Floudas, D., Binder, M., Majcherczyk, A., Schneider, P., Aerts, A., Asiegbu, F.O., Baker, S.E., Barry, K., Bendiksby, M., Blumentritt, M., Coutinho, P.M., Cullen, D., de Vries, R.P., Gathman, l., Goodell, B., Henrissat, B., Ihrmark, K., Kauserud, H., Kohler, A., LaButti, K., Lapidus, A., Lavin, J.L., Lee, Y.-H., Lindquist, E., Lilly, W., Lucas, S., Morin, E., Murat, C., Oguiza, J.A., Park, J., Pisabarro, A.G., Riley, R., Rosling, A., Salamov, A., Schmidt, O., Schmutz, J., Skrede, I., Stenlid, J., Wiebenga, A., Xie, X., Kües, U., Hibbett, D.S., Hoffmeister, D., Högberg, N., Martin, F., Grigoriev, I.V., Watkinson, S.C., 2011. The plant cell wall–decomposing machinery underlies the functional diversity of forest fungi. Science 333(6043), 762-765.

Filley, T.R., Cody, G.D., Goodell, B., Jellison, J., Noser, C., Ostrofsky, A., 2002. Lignin demethylation and polysaccharide decomposition in spruce sapwood degraded by brown rot fungi. Organic Geochemistry 33(2), 111-124.

Flournoy, D.S., Kirk T.K., Highley T., 1991. Wood decay by brown-rot fungi: changes in pore structure and cell wall volume. Holzforschung, 45(5), 383-8.

Floudas, D., Binder, M., Riley, R., Barry, K., Blanchette, R.A., Henrissat, B., Martínez, A.T., Otillar, R., Spatafora, J.W., Yadav, J.S., Aerts, A., Benoit, I., Boyd, A., Carlson, A., Copeland, A., Coutinho, P.M., de Vries, R.P., Ferreira, P., Findley, K., Foster, B., Gaskell, J., Glotzer, D., Górecki, P., Heitman, J., Hesse, C., Hori, C., Igarashi, K., Jurgens, J.A., Kallen, N., Kersten, P., Kohler, A., Kües, U., Kumar, T.K., Kuo, A., LaButti, K., Larrondo, L.F., Lindquist, E., Ling, A., Lombard, V., Lucas, S., Lundell, T., Martin, R., McLaughlin, D.J., Morgenstern, I., Morin, E,, Murat, C., Nagy, L.G., Nolan, M., Ohm, R.A., Patyshakuliyeva, A., Rokas, A., Ruiz-Dueñas, F.J., Sabat, G., Salamov, A., Samejima, M., Schmutz, J., Slot, J.C., St John, F., Stenlid, J., Sun, H., Sun, S., Syed, K., Tsang, A., Wiebenga, A., Young, D., Pisabarro, .A, Eastwood, D.C., Martin, F., Cullen, D., Grigoriev, I.V., Hibbett, D.S., 2012. The Paleozoic origin of enzymatic lignin decomposition reconstructed from 31 fungal genomes. Science 336(6089), 1715-1759.

Goldstein, I.S., Jeroski, E.B., Lund, A.E., Nielson, J.F., Weaver, J.W., 1961. Acetylation of wood in lumber thickness. Forest Products Journal 11, 363-370.

Goodell, B., Jellison, J., Liu, J., Daniel, G., Paszczynski, A., Fekete, F., Krishnamurthy, S., Jun, L., Xu, G. 1997. Low molecular weight chelators and phenolic compounds

isolated from wood decay fungi and their role in the fungal biodegradation of wood. Journal of Biotechnology 53, 133-162.
Goodell, B., Zhu, Y., Kim, S., Kafle, K., Eastwood, D., Daniel, G., Jellison, J., Yoshida, M., Groom, L., Pingali, S.V., O'Neill, H. (2017). Modification of the nanostructure of lignocellulose cell walls via a non-enzymatic lignocellulose deconstruction system in brown rot wood-decay fungi. Biotechnology for Biofuels *10*, 179.
Green III, F., Clausen, C.A., Larsen, M. J., & Highley, T.L. (1992). Immuno-scanning electron microscopic localization of extracellular wood-degrading enzymes within the fibrillar sheath of the brown-rot fungus Postia placenta. Canadian Journal of Microbiology 38(9), 898–904.
Green III, F., Kuster, T.A., Highley, T.L. (1996). Pectin degradation during colonization of wood by brown-rot fungi. Recent Research Developments in Plant Pathology 1, 83-93.
Hemsworth, G.R., Johnston, E.M., Davies, G.J., Walton, P.H., 2015. Lytic polysaccharide monooxygenases in biomass conversion. Trends in biotechnology 33(12), 747-761.
Hill, C.A.S., 2006. Wood Modification: Chemical, Thermal and Other Processes. John Wiley & Sons.
Hill, C.A.S., Forster, S.C., Farahani, M.R.M., Hale, M.D.C., Ormondroyd, G.A., Williams, G.R., 2005. An investigation of cell wall micropore blocking as a possible mechanism for the decay resistance of anhydride modified wood. International Biodeterioration & Biodegradation 55(1), 69–76.
Hill, C.A.S., Hale, M.D., Ormondroyd, G.A., Kwon, J.H., Forster, S.C., 2006. Decay resistance of anhydride-modified Corsican pine sapwood exposed to the brown-rot fungus *Coniophora puteana*. Holzforschung 60, 625-629.
Irbe, I., Andersons, B., Chirkova, J., Kallavus, U., Andersone, I., Faix, O., 2006. On the changes of pinewood (*Pinus sylvestris* L.) Chemical composition and ultrastructure during the attack by brown-rot fungi *Postia placenta* and *Coniophora puteana*. International Biodeterioration & Biodegradation 57(2), 99–106.
Jensen Jr., K.A., Ryan, Z.C., Wymelenberg, A.V., Cullen, D., Hammel, K.E., 2002. An NADH: quinone oxidoreductase active during biodegradation by the brown-rot basidiomycete *Gloeophyllum trabeum*. Applied and environmental microbiology 68(6), 2699-703.
Kersten, P., Cullen, D., 2014. Copper radical oxidases and related extracellular oxidoreductases of wood-decay Agaricomycetes. Fungal Genetics and Biology 72, 124-130.
Kim, Y.S., Goodell, B., & Jellison, J. 2009. Immuno-electron microscopic localization of extracellular metabolites in spruce wood decayed by brown-rot fungus *Postia placenta*. Holzforschung 45(5), 389–393.
Kumar, S., Agarwal, S.C., 1983. Biological degradation resistance of wood acetylated with thioacetic acid. IRG/WP 83-3223. The International Research Group on Wood Protection. Stockholm, Sweden.
Levasseur, A., Drula, E., Lombard, V., Coutinho, P.M., Henrissat, B., 2013. Expansion of the enzymatic repertoire of the CAZy database to integrate auxiliary redox enzymes. Biotechnology for biofuels 6(1), 41.
Li, X.L., Skory, C.D., Cotta, M.A., Puchart, V., Biely, P., 2008. Novel family of carbohydrate esterases, based on identification of the Hypocrea jecorina acetyl esterase gene. *Applied and environmental microbiology*, *74*(24), 7482-7489.

Lombard, V., Golaconda, Ramulu, H., Drula, E., Coutinho, P.M., Henrissat, B., 2013. The carbohydrate-active enzymes database (CAZy) in 2013. Nucleic Acids Research 42(1), 490-5.

Martinez, D., Challacombea, J., Morgensternc, I., Hibbettc, D., Schmolld, M., Kubicekd, C.P., Ferreirae, P., Ruiz-Duenase, F.J., Martineze, A.T., Kerstenf, P., Hammelf, K.E., Vanden Wymelenberg, A., Gaskellf, J., Lindquisth, E., Sabati, G., BonDuranti, S.S., Larrondoj, L.F., Canessaj, P., Vicunaj, R., Yadavk, J., Doddapanenik, H., Subramaniank, V., Pisabarrol, A. G., Lavínl, J.L., Oguizal, J.A., Masterm, E., Henrissatn, B., Coutinhon, P.M., Harriso, P., Magnusonp, J.K., Bakerp, S.E., Brunop, K., Kenealyq, W., Hoegger, P.J., Kuesr, U., Ramaiyao, P., Lucash, S., Salamovh, A., Shapiroh, H., Tuh, H., Cheeb, C.L., Misraa, M., Xiea, G., Tetero, S., Yavero, D., Jamess, T., Mokrejst, M., Pospisekt, M., Grigorievh, I.V., Brettina, T., Rokhsarh, D., Berkao, R., Cullenf, D., 2009. Genome, transcriptome, and secretome analysis of wood decay fungus *Postia placenta* supports unique mechanisms of lignocellulose conversion. Proceedings of the National Academy of Sciences, 106(6), 1954-1959.

Mohebby, B., 2003. Biologicial attack of acetylated wood. PhD Thesis. Institute of Wood Biology and Wood Technology. Georg-August-Universität Göttingen. Göttingen, Germany.

Niemenmaa, O., Uusi-Rauva, A., Hatakka, A., 2008. Demethoxylation of [O 14 CH 3]-labelled lignin model compounds by the brown-rot fungi *Gloeophyllum trabeum* and *Poria* (*Postia*) *placenta*. Biodegradation 19(4), 555.

Olaru, N., Olaru, L., Vasile, C., Ander, P. (2011). Surface modified cellulose obtained by acetylation without solvents of bleached and unbleached kraft pulps. Polimery, 56.

Pan, X., Gilkes, N., Saddler, J.N. 2006. Effect of acetyl groups on enzymatic hydrolysis of cellulosic substrates. Holzforschung, 60(4), 398-401.

Papadopoulos, A.N., Hill, C.A.S., 2002. The biological effectiveness of wood modified with linear chain carboxylic acid anhydrides against *Coniophora puteana*. Holz Als Roh-und Werkstoff 60, 329-332.

Papadopoulos, A.N., Hill, C.A.S., 2003. The sorption of water vapour by anhydride modified softwood. Wood Science and Technology, 37(3–4), 221–231.

Passarini, L., Zelinka, S.L., Glass, S.V., Hunt, C.G., 2017. Effect of weight percent gain and experimental method on fiber saturation point of acetylated wood determined by differential scanning calorimetry. Wood Science and Technology, 51(6), 1291–1305.

Paszczynski, A., Crawford, R., Funk, D., Goodell B., 1999. De Novo Synthesis of 4, 5-Dimethoxycatechol and 2, 5-Dimethoxyhydroquinone by the Brown Rot Fungus *Gloeophyllum trabeum*. Applied and Environmental Microbiology, 65(2), 674-9.

Peterson, M.D., Thomas, R.J., 1978. Protection of wood from decay fungi by acetylation – an ultrastructural and chemical study. Wood and Fiber Science, 10, 149-163.

Pilgård, A., Schmöllerl, B., Risse, M., Fossdal, C.G,, Alfredsen, G., 2017. Profiling *Postia placenta* colonization in modified wood – microscopy, DNA quantification and gene expression. 13th Annual Meeting of the Northern European Network for Wood Science and Engineering (WSE 2017). September 28-29, University of Copenhagen, Denmark. 6 p.

Popescu, C. M., Hill, C.A.S., Curling, S., Ormondroyd, G., & Xie, Y. (2014). The water vapour sorption behaviour of acetylated birch wood: how acetylation affects the sorption isotherm and accessible hydroxyl content. Journal of materials science 49(5), 2362-2371.

946 Presley, G.N., Zhang, J, Schilling, J.S., 2016. A genomics-informed study of oxalate and
947 cellulase regulation by brown rot wood-degrading fungi. Fungal Genetics and
948 Biology, 12, 64-70.
949 Riley, R., Salamov, A.A., Brown, D.W., Nagy, L.G., Floudas, D., Held, B.W., Levasseur,
950 A., Lombard, V., Morin, E., Otillar, R., Lindquist, E.A., Sun, H., LaButti, K.M.,
951 Schmutz, J., Jabbour, D., Luo, H., Baker, S.E., Pisabarro, A.G., Walton, J.D.,
952 Blanchette, R.A., Henrissat, B., Martin, F., Cullen, D., Hibbett, D.S., Grigoriev,
953 I.V., (2014). Extensive sampling of basidiomycete genomes demonstrates
954 inadequacy of the white-rot/brown-rot paradigm for wood decay fungi.
955 Proceedings of the National Academy of Sciences 111(27), 9923-8.
956 Ringman, R., Pilgård, A., Brischke, C., Richter, K., 2014a. Mode of action of brown rot
957 decay resistance in modified wood: a review. Holzforschung 68, 239-246.
958 Ringman, R., Pilgård, A., Brischke, C., Windeisen, E., Richter, K., 2017. Incipient brown
959 rot decay in modified wood: patterns of mass loss, structural integrity, moisture
960 and acetyl content in high resolution. International Wood Products Journal 8(3),
961 172–182.
962 Ringman, R., Pilård, A., Richter, K., 2014b. Effect of wood modification on gene
963 expression during incipient *Postia placenta* decay. International Biodeterioration
964 & Biodegradation, 86, 86-91.
965 Ringman, R., Pilgård, A., Richter, K., 2015. In vitro oxidative and enzymatic degradation
966 of modified wood. International Wood Products Journal 6(1), 36-39.
967 Rose, J. K., Bennett, A. B., 1999. Cooperative disassembly of the cellulose–xyloglucan
968 network of plant cell walls: parallels between cell expansion and fruit ripening.
969 Trends in plant science 4(5), 176-183.
970 Rowell, R.M., 2005. Handbook of Wood Chemistry and Wood Composites. CRC Press.
971 Sützl, L., Laurent, C. V., Abrera, A. T., Schütz, G., Ludwig, R., Haltrich, D., 2018.
972 Multiplicity of enzymatic functions in the CAZy AA3 family. Applied
973 microbiology and biotechnology 102(6), 2477-2492.
974 Smith, K.T., Shortle, W.C., Jellison, J., Connolly, J., Schilling, J., 2007. Concentrations
975 of Ca and Mg in early stages of sapwood decay in red spruce, eastern hemlock,
976 red maple, and paper birch. Canadian journal of forest research 37(5), 957-965.
977 Schilling, J.S., Bissonnette, K. M., 2008. Iron and calcium translocation from pure
978 gypsum and iron-amended gypsum by two brown rot fungi and a white rot
979 fungus. Holzforschung, 62(6), 752-758.
980 Takahashi, M., Imamura, Y., Tanahashi, M., 1989. Effect of acetylation on decay
981 resistance of wood against brown-rot, white-rot and soft-rot fungi. IRG/WP 89-
982 3540. International Research Group on Wood Protection. Stockholm, Sweden.
983 Tschernitz, J.L., Sachs, I.B., 1975. Observations on microfibril organization of Douglas-
984 fir bordered pit-pair membranes by scanning electron microscopy. Wood and
985 Fiber Science 6(4), 332-340.
986 Thybring, E. E. 2017. Water relations in untreated and modified wood under brown-rot
987 and white-rot decay. International Biodeterioration & Biodegradation 118, 134-
988 142.
989 Waterham, H.R., Russell, K.A., De Vries, Y., Cregg, J.M., 1997. Peroxisomal targeting,
990 import, and assembly of alcohol oxidase in *Pichia pastoris*. The Journal of Cell
991 Biology 139(6), 1419-1431.
992 Winandy, J. E., Morrell, J. J., 1993. Relationship between incipient decay, strength, and
993 chemical composition of Douglas-fir heartwood. Wood and Fiber Science 25(3),
994 278-288.

995 Xu, G., Goodell, B., 2001. Mechanisms of wood degradation by brown-rot fungi:
996 chelator-mediated cellulose degradation and binding of iron by cellulose. Journal
997 of biotechnology, 87(1), 43-57.
998 Yelle D.J., Wei D., Ralph J., Hammel K.E., 2011. Multidimensional NMR analysis
999 reveals truncated lignin structures in wood decayed by the brown rot
1000 basidiomycete *Postia placenta*. Environmental Microbiology 13, 1091-1100.
1001 Zabel, R. A., Morrell, J. J., 1992. Wood Microbiology: Decay and Its Prevention.
1002 Academic Press.
1003 Zhang, J., Presley, G N., Hammel, K.E., Ryu, J.S., Menke, J.R., Figueroa, M., Hu, D.,
1004 Orr, G., Schilling, J.S., 2016. Localizing gene regulation reveals a staggered wood
1005 decay mechanism for the brown rot fungus *Postia placenta*. Proceedings of the
1006 National Academy of Sciences 113(39), 10968-10973.
1007 Zhang, J., Schilling, J.S., 2017. Role of carbon source in the shift from oxidative to
1008 hydrolytic wood decomposition by *Postia placenta*. Fungal Genetics and Biology
1009 106, 1-8.
1010 Zhang, J., Siika-aho, M., Tenkanen, M., Viikari, L., 2011. The role of acetyl xylan
1011 esterase in the solubilization of xylan and enzymatic hydrolysis of wheat straw
1012 and giant reed. Biotechnology for Biofuels 4(1), 60.
1013

1014 **Tables and figures**

1015

Gene (abbreviation)	Protein id	Function	Forward primer/ reverse primer
1: Genes involved in oxidative depolymerisation			
1.1: Oxalate synthesis and oxalate decomposition			
Glyoxylate dehydrogenase (GlyD)	121561	Involved in oxalate synthesis	CGGAGCTGGACCTTTGTTAC/ GCGCGAAGGCAAATCTAATA
Oxaloacetate acetylhydrolase (OahA)	112832	Involved in oxalate synthesis	AAGGCGTTCTTCGAGGTCAT/ AAAGCAGCAACCCGAGAAG
Oxalate decarboxylase (OxaD)	43912	Involved in oxalate decomposition	GAACCTATAACTACGAGGCAAGC/ CCAGGAATACCAGAGGCTCA
1.2: Redox enzymes			
AA3 GMC oxidoreductase (AOx1)	44331	Involved in oxidative depolymerisation Possible H_2O_2 source	GGAGGTACAGACGGACGAAC/ AGAGTCGACGACACCGTTCT
AA3 GMC oxidoreductases (AOx2)	129158	Most likely involved in oxidative depolymerisation Possible H_2O_2 source	TACTCGACGGCCCTCACTAT/ CCGCTTGAGACTGAACACTG
AA3 GMC oxidoreductase (AOx3)	118723	Involved in oxidative depolymerisation Likely source of H_2O_2	ACACCAAGGAGGACGACGAG/ GACGAGCAAGGCAGACGAGTA
Copper radical oxidase (Cro1)	56703	Involved in oxidative depolymerisation Likely source of H_2O_2	CGGCGATGTTTCGGACGTTAT/ CCGCCATTCCAATAGTAGAGC
Copper radical oxidase (Cro2)	104114	Involved in oxidative depolymerisation Likely source of H_2O_2	CGCAGACGATGGAGGTGGTC/ GTGACACCGCACCGTTACCA
Benzoquinone reductases (BqR)	12517	Involved in oxidative depolymerisation Possibly involved in reduction of chelator/ reductants	CGTACAAAGAACGCCCTCTC/ GTGGCCGTACATGGAGTAGA
2: Hydrolytic enzymes involved in polysaccharide depolymerisation and LPMO			
2.1: Cellulose degradation			
GH5 Endoglucanase (Cel5a)	115648	Major endocellulase	TTCTGTCCATGACACCGTACA/ TCCTCTTGGTGTAGGTCCGTA
GH5 Endoglucanase (Cel5b)	103675	Major endocellulase	CTCGCATACGTGCAATCG/ GGAGTAGGGCGTCACAGAGA
GH12 Glucoside hydrolase (Cel12a)	121191	Endoglucanase active on cellulose and/or xyloglucan	TCAACGTCGAGAGCTTCAG/ GACGAAGAGCTAAGGACACCA
GH3 Betaglucosidase (bGlu)	128500	Hydrolyses cellobiose, releasing glucose	AGGCACAAGCCAAGTCGTCA/ CTTGGCAATCGTGAAAGTGGT
AA9 Lytic polysaccharide monooxygenases (LPMO)	126811	Polysaccharide depolymerisation via oxidative cleavage of glycosidic bonds	GCCAGATATCACGGTCACCT/ TCGTAGATGTCGGGAACGTA
2.2: Hemicellulose and pectin degradation			
GH5 Endomannanase (Man5a)	121831	Involved in glucomannan depolymerisation, highly expressed	GCTGACTGGCACCGACTACC/ CCCACGAACGCATCCAAATAG
GH10 Endoxylanase (Xyl10a)	113670	Involved in xylose depolymerisation	CTTCGGCTCTGCTACGGACAA/ ACCATACGCAGTTGTGTCCTCT
GH10b Endoxylanase (Xyl10b)	105534	Involved in xylose depolymerisation	TCGGAGCCTGAGCCATTTGT/ TGCTGCGGTGTAATTGTTGG

GH3 Beta xylosidase (bXyl)	51213	Hemicellulose depolymerisation	GTGCGTTTCCCGACTGTGC/ GCGGTGTTGCCGGTATTGT
Carbohydrate esterase (CE16a)	125801	Deacetylation of carbohydrates	ACACCGTGCACAACATCCT/ CGTGCTCCAAGTCTGATGAT
GH28 Polygalacturonase (Gal28a)	111730	Involved in pectin depolymerisation	CCGGCAATACAATTTCTGGCA/ GTTCCGGGAGTACCGTCATT
3: Expansins			
Expansin (Exp1)	126976	Most likely involved in increasing enzyme accessibility	TGTCGGAATGAGCGGTCT/ ATGCATGAACCGCCTTTGT
Expansin (Exp2)	128179	Most likely involved in increasing enzyme accessibility	AATGTGACTTGGGCCATTGT/ AATACCGTGCAAGCGTCAGT
4: Housekeeping			
α-tubulin (αt)	123093	Major component of the eukaryotic cytoskeleton	GGAGTCGCCTTGACCACAA/ TGCCCTCACCAACGTACCA
β-tubulin (βt)	113871	Major component of the eukaryotic cytoskeleton	CAGGATCTTGTCGCCGAGTAC/ CCTCATACTCGCCCTCCTCTT

Table 1. qRT-PCR primers: gene (abbreviation), JGI protein id for *Rhodonia placenta*, function, forward and reverse primer.

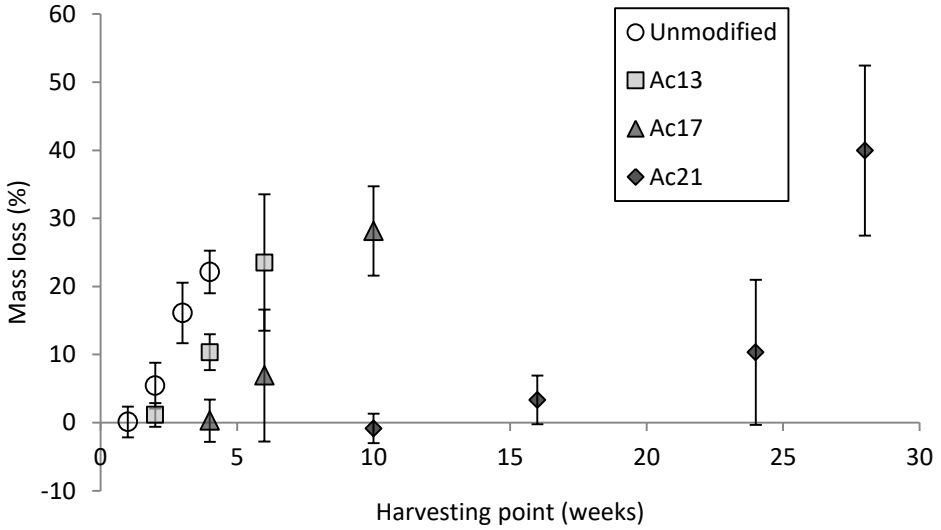

Figure 1: Mass loss in percent for *Pinus radiata* (unmodified) and acetylated samples with WPG 13 (Ac13), WPG17 (Ac17) and WPG 21 (Ac21) at different harvesting points (weeks).

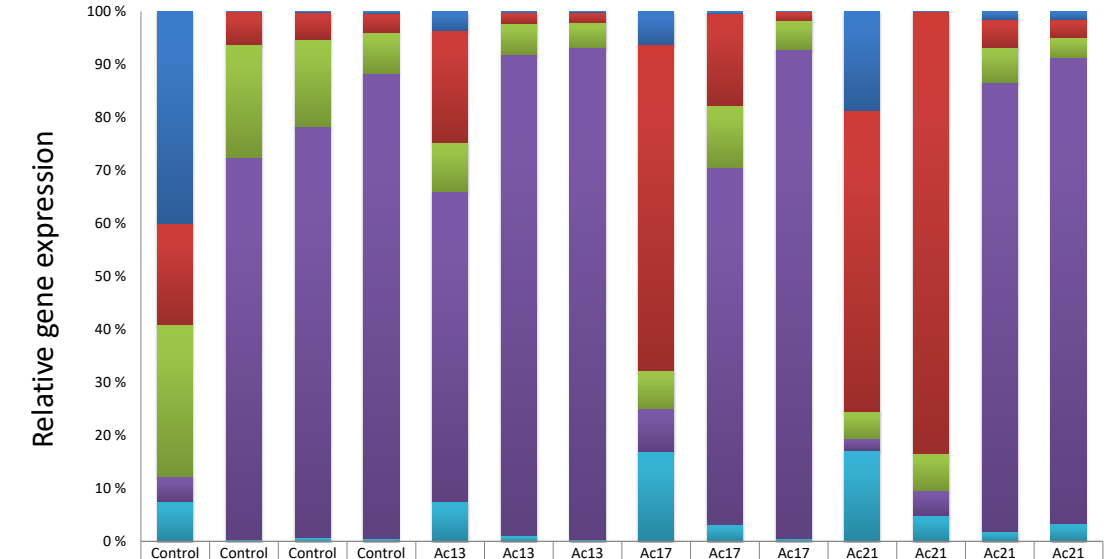

	Control week 1	Control week 2	Control week 3	Control week 4	Ac13 week2	Ac13 week 4	Ac13 week 6	Ac17 week4	Ac17 week6	Ac17 week10	Ac21 week 10	Ac21 week 16	Ac21 week 24	Ac21 week 28
Oxalate synthesis	12904	283	711	2088	8211	1828	1953	5336	1414	582	8067	278	5813	5777
Oxidative	6148	26524	31552	25405	48208	23136	33559	52467	65676	17568	24357	290476	20403	12939
Hemicellulolytic	9259	92267	101997	53603	21045	65948	77126	6159	44178	58905	2173	24286	25537	14324
Cellulolytic	1511	310489	479679	606412	133266	1028376	1535878	6824	253281	983356	975	16648	328117	331314
Expansins	2437	1898	4131	3677	16974	11953	6635	14502	12313	6507	7399	17185	7154	12846

Figure 2: Relative expression of 22 *R. placenta* genes during decay of unmodified and acetylated (13, 17 and 21% WPG) *Pinus radiata* earlywood. The units given are arbitrary gene expression units, in relation to the constitutive beta-tubulin gene with an expression level of 10^4. Note that the sum total expression level varies between harvesting points and treatment levels.

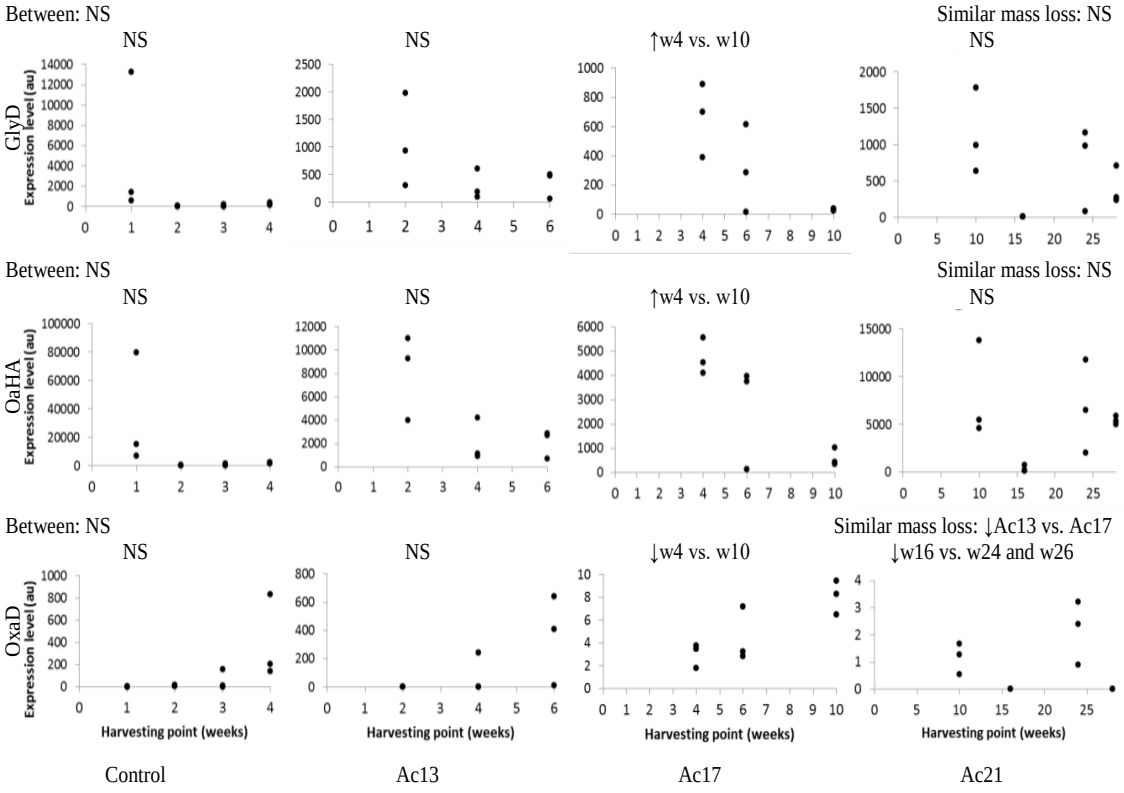

Figure 3: Oxalate synthesis (glyoxylate dehydrogenase, GlyD Ppl125161, oxaloacetate dehydrogenase OahA, Ppl112832) and oxalate decomposition (oxalate decarboxylase OxaD Ppl43912) at different harvesting points (weeks). Tukey's HSD comparisons are provided between treatments (top row left), between treatments at the first harvesting point (top row right), and within treatments (second row).

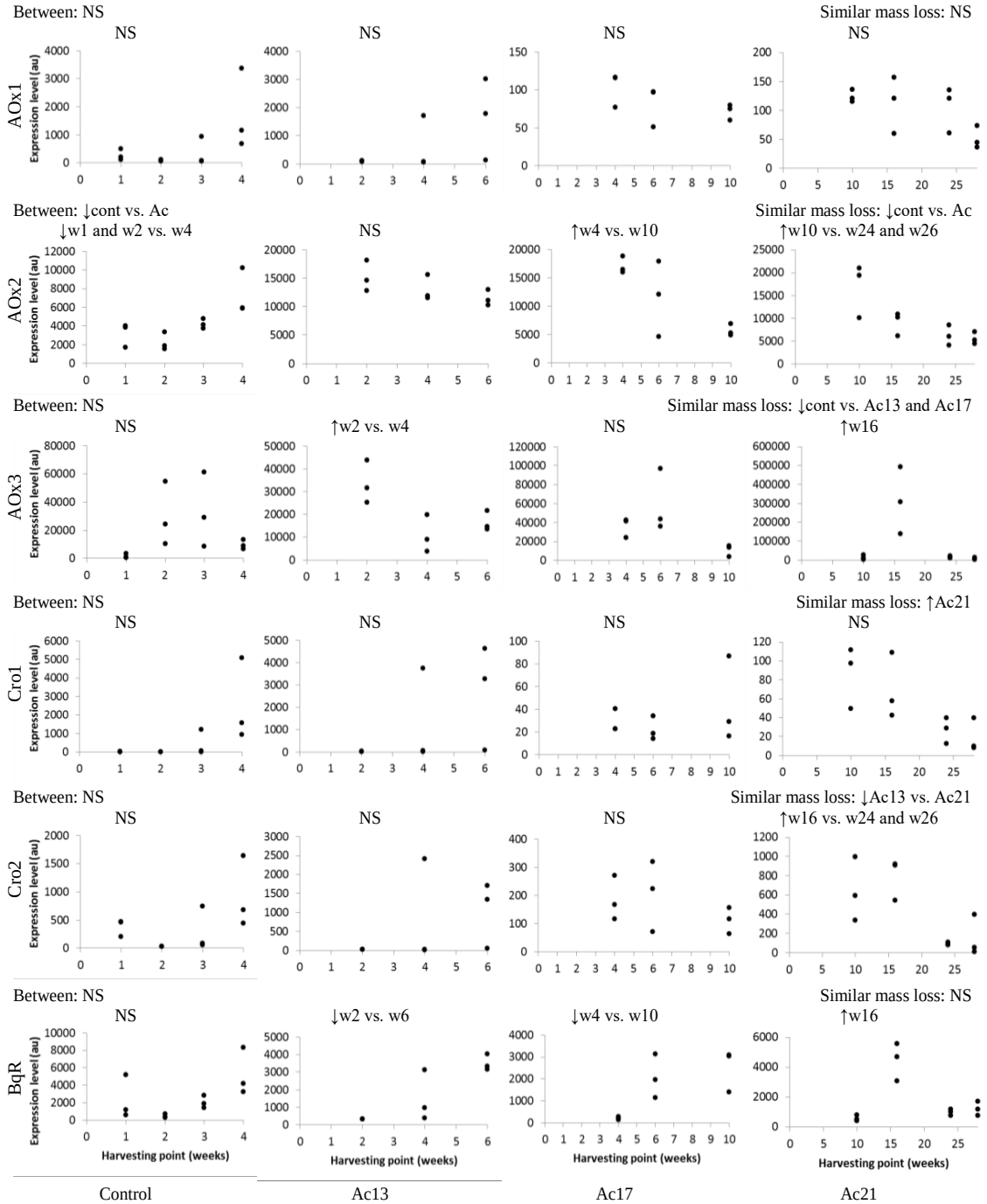

Figure 4: Redox enzymes at different harvesting points (weeks). Tukey's HSD comparisons are provided between treatments (top row left), between treatments at the first harvesting point (top row right), and within treatments (second row).

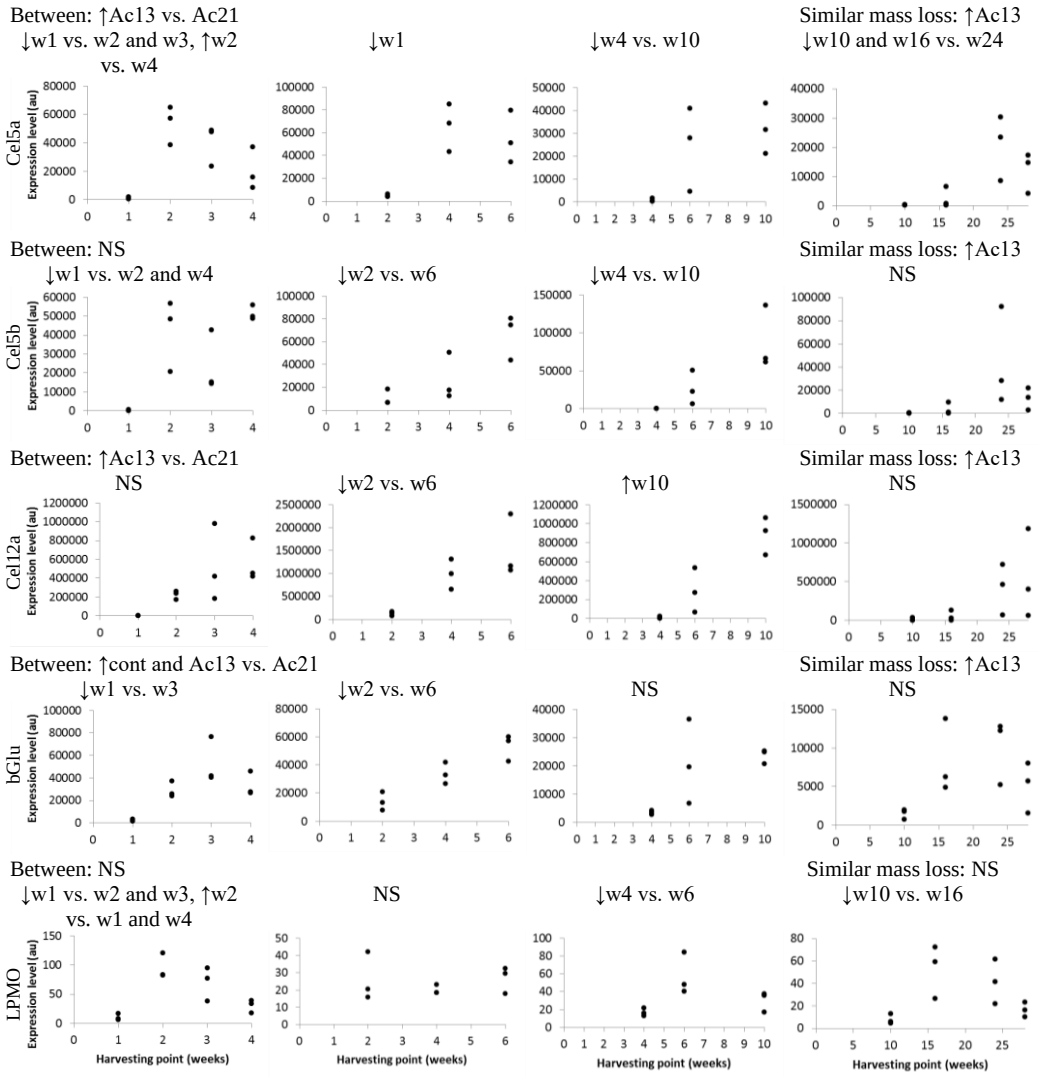

Figure 5: Cellulose degrading enzymes at different harvesting points (weeks). Tukey's HSD comparisons are provided between treatments (top row left), between treatments at the first harvesting point (top row right), and within treatments (second row).

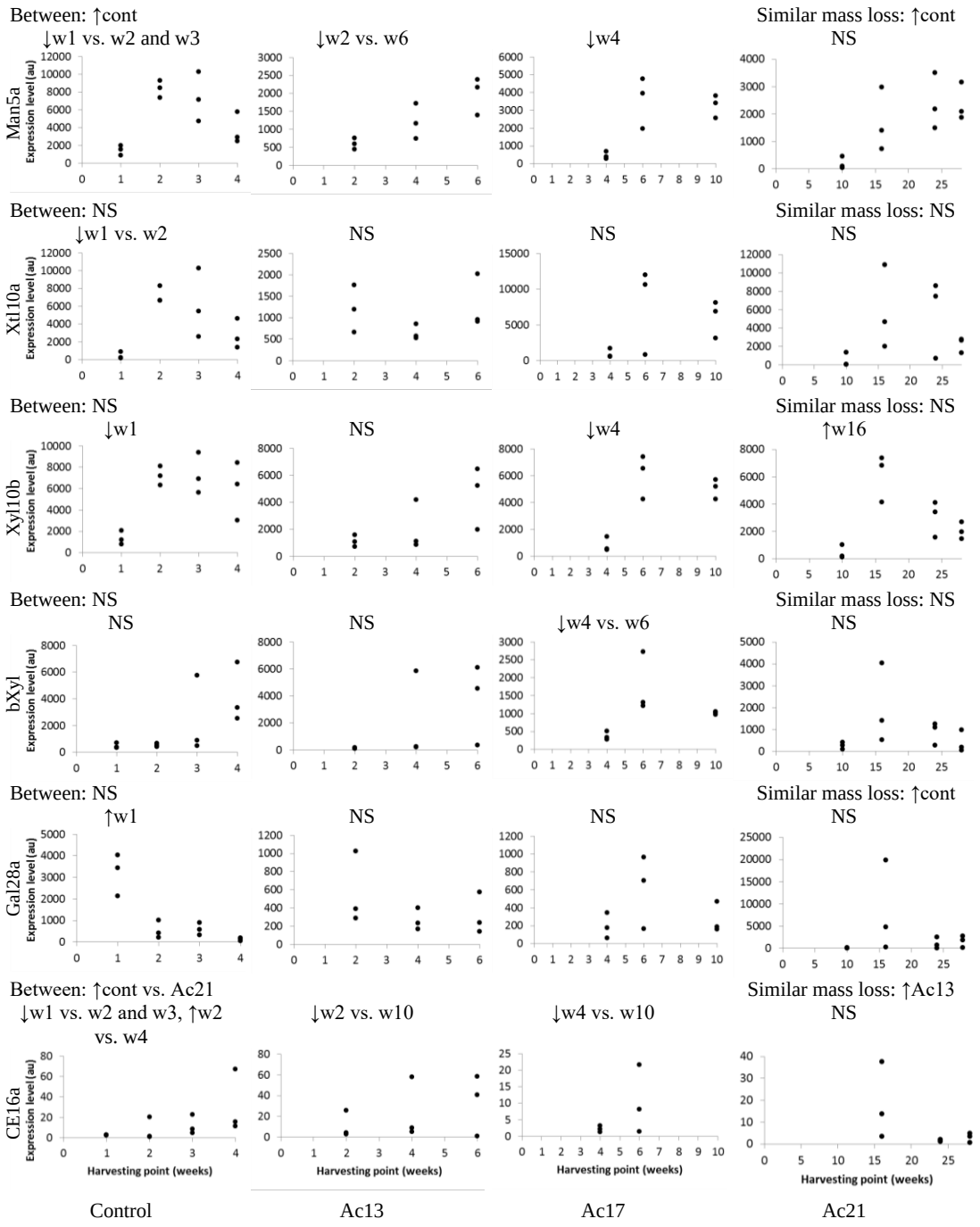

Figure 6: Hemicellulose and pectin degrading enzymes at different harvesting pints (weeks). Tukey's HSD comparisons are provided between treatments (top row left), between treatments at the first harvesting point (top row right), and within treatments (second row).

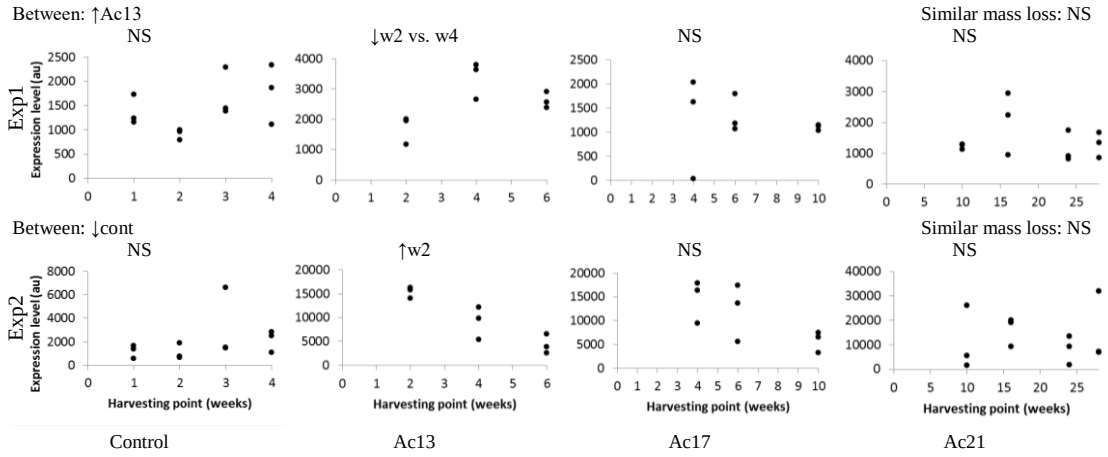

Figure 7: Expansin enzymes at different harvesting pints (weeks). Tukey's HSD comparisons are provided between treatments (top row left), between treatments at the first harvesting point (top row right), and within treatments (second row).